Structure and Dynamics in Oligomannose-Type Oligosaccharides†

S. W. Homans,* A. Pastore, R. A. Dwek, and T. W. Rademacher

Department of Biochemistry, University of Oxford, Oxford OX1 3QU, England

Received April 15, 1987; Revised Manuscript Received June 8, 1987

ABSTRACT: Using a combination of ^{1}H NMR nuclear Overhauser effect measurements, molecular orbital calculations, and molecular dynamics simulations, we have determined the tertiary structure and dynamic properties of the oligomannose oligosaccharide Manα6(Manα3)Manα6(Manα3)Manβ4GlcNAcβ4GlcNAc. While the calculated potential surfaces for the majority of the glycosidic linkages could be described by a single deep potential well, similar calculations for the Manα1–6Manα and Manα1–6Manβ linkages described a diffuse, shallow well, suggesting that a larger degree of flexibility exists about the latter. These conclusions are supported by the results of molecular dynamics simulations, which suggest that the NMR data should be interpreted in terms of a degree of flexibility about the Manα1–6Manβ and Manα1–6Manα linkages. In contrast, a similar series of investigations suggests that the conformation of the Manα1–6Manβ linkage in Manα2Man6(Manα2Manα3)Manα6(Manα2Manα2Manα3)Manβ4GlcNAcβ4GlcNAc is more restricted, resulting in an overall structure that is "restrained".

High-resolution ^{1}H nuclear magnetic resonance is a well-established method for the derivation of the three-dimensional structures of biomolecules in solution. The use of two-dimensional coherence-transfer methods such as ^{1}H–^{1}H correlated spectroscopy, together with ^{1}H–^{1}H nuclear Overhauser effect spectroscopy, can generate sufficient through-bond and through-space connectivity information to allow the complete determination of the three-dimensional structure of small noncrystalline proteins (Wüthrich et al., 1982). A similar series of experiments, together with semiempirical molecular orbital calculations, can be used to determine the solution conformations of glycoprotein oligosaccharides (Homans et al., 1986). While several investigations of glycoprotein oligosaccharide conformations have been reported, none of these has, in general, addressed the question of the dynamics of these conformations (Homans et al., 1982, 1986; Bock et al., 1982; Brisson & Carver, 1983a,b; Paulsen et al., 1984, 1986; Biswas et al., 1987). Although conformational averaging in N-linked oligosaccharides is well documented, available evidence suggests that this is restricted to transitions about the C5–C6 bond of Manα1–6Manβ and Manα1–6Manα linkages, where the presence of more than one stable conformer can be theoretically predicted and confirmed experimentally from ^{1}H NMR[1] spin-coupling constant data (Homans et al., 1986). Furthermore, it is well-known that the use of ^{1}H NMR nuclear Overhauser effect (NOE) measurements to obtain distance constraints defines an average conformation on the NMR time scale. This might suggest that the NMR-derived structure represents an average of several unique conformers or is weighted heavily in favor of a single conformer that bears little relation to the actual structure by virtue of the dependence of the NOE upon the inverse sixth power of the internuclear distance [see, e.g., Jardetzky and Roberts (1981)]. To a certain extent this can be assessed from the magnitude of the NOE together with theoretical molecular orbital calculations. For example, in a recent study upon the solution conformations of Manα1–3Manβ linkages in a variety of N-linked oligosaccharides (Homans et al., 1987), both experimental and theoretical data were weighted heavily against the presence of more than one conformer about the Manα1–3Manβ linkage for any given oligosaccharide. In brief, the NMR-derived conformation was found to be in good agreement with that computed from molecular orbital calculations, which predicted a single deep potential well. In addition, the measured NOE's were close to their theoretical maximum values, which ruled out the presence of a highly populated alternative conformer. However, even with due consideration to these constraints, it is not possible given the nature of the NOE data to describe the Manα1–3Manβ linkage as "rigid", and narrow torsional oscillations about the experimentally derived conformation (i.e., within the potential well) must be considered likely. In principle, NMR relaxation measurements might provide additional insight into the relative "flexibility" of glycosidic linkages, but since the system remains undefined in the case of motional anisotropy (e.g., with regard to the number and/or geometry of alternative conformers), these measurements would not be amenable to meaningful interpretation. An alternative approach is to model the dynamics of the system by simulation of molecular dynamics trajectories. This approach has been shown to be of great value in the interpretation of NMR measurements in proteins (Hoch et al., 1985) but to our knowledge has not been applied to glycoprotein oligosaccharides.

In this paper, using a combination of ^{1}H NMR nuclear Overhauser effect measurements, molecular orbital calculations, and molecular dynamics simulations, we estimate the magnitude of such torsional oscillations about the glycosidic linkages in the oligomannose-type oligosaccharides I and II (Figure 1). We have chosen these compounds since compound II has conformational flexibility about the C5–C6 bond of Man-3, whereas compound I is restricted to a single rotamer about this bond (Homans et al., 1986). A detailed comparison of structure and dynamics between these compounds thus allows for a fuller description of the solution conformation(s)

† This work is a contribution from the Oxford Oligosaccharide Group, which is supported by Monsanto. S.W.H., R.A.D., and T.W.R. are members of the Oxford Enzyme Group.

[1] Abbreviations: NMR, nuclear magnetic resonance; NOE, nuclear Overhauser effect; NOESY, two-dimensional nuclear Overhauser effect spectroscopy; MNDO, modified neglect of diatomic differential overlap; MD, molecular dynamics.

0006-2960/87/0426-6649$01.50/0 © 1987 American Chemical Society

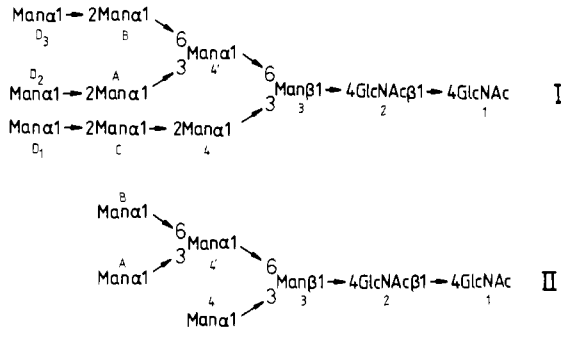

FIGURE 1: Structures of the compounds described in this study.

of a structure which is presumed to be restrained (I) and a structure which can be described in terms of additional localized flexibility (II).

Materials and Methods

Compounds I and II (Figure 1) were released from soybean agglutinin (Dorland et al., 1981) and bovine pancreatic ribonuclease (Liang et al., 1980), respectively, by large-scale hydrazinolysis, followed by purification on Bio-Gel P-4 (−400 mesh). Compound I eluted at 12.3 glucose units, and compound II eluted at 8.4 glucose units.

NMR Spectroscopy. Two-dimensional ^1H–^1H phase-sensitive nuclear Overhauser effect (NOESY) experiments were performed as described previously, together with a general assignment strategy for compounds such as I and II (Homans et al., 1986, 1987).

Energy Calculations. Stable conformers of the model compounds Manα1–2Manα, Manα1–3Manα, Manα1–6Manβ, and Manα1–6Manα were determined with molecular orbital (MNDO) procedures by complete optimization of bond lengths, bond angles, and torsional angles in each compound with the AMPAC molecular orbital package (Dewar & Stewart, 1986) as described previously (Homans et al., 1986, 1987). Ring carbon atoms in the model compounds are designated clockwise C1 to C5, with C1 being the anomeric carbon. The ring oxygen is designated O5. The remaining hydrogen and oxygen atoms are labeled according to their parent carbon atoms, with hydroxyl protons designated H′. The dihedral angles about the glycosidic linkages are defined as ϕ = C1–O1–CX–HX and ψ = C2–C1–O1–CX, where CX and HX are the aglyconic atoms. In the case of 1–6 linkages, ϕ = C1–O1–C6–C5.

Molecular Dynamics Simulations. Molecular dynamics simulations on Manα1–3Manβ and Manα1–6Manα were performed with the GROMOS package (van Gunsteren & Berendsen, 1977; van Gunsteren & Karplus, 1982; van Gunsteren et al., 1983). All atoms were treated explicitly, except for hydrogen atoms bound to carbon atoms. These are incorporated into the latter forming united atoms. The inital configuration was energy minimized with the AMPAC molecular orbital package. Initial velocities for the atoms were taken from a Maxwellian distribution at 300 K, and the system was weakly coupled to a thermal bath, T_0 = 300 K. The MD run covered a time span of 12 ps, of which the last 10 ps was used for analysis.

Results

The correct conditions by which quantitative distance information can be obtained from two-dimensional ^1H–^1H nuclear Overhauser effect (NOESY) measurements on compounds I and II have been described in detail elsewhere (Homans et al., 1987). Here, we provide a complete analysis

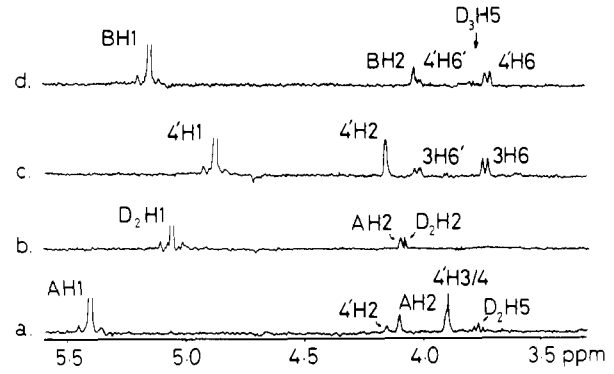

FIGURE 2: Cross-sections through the NOESY spectrum of structure I (Figure 1) with (a) Man-A H1 on the diagonal, (b) Man-D_2 H1 on the diagonal, (c) Man-4′ H1 on the diagonal, and (d) Man-B H1 on the diagonal.

of the interresidue and intraresidue NOE connectivities between residues in the Manα1–3 and Manα1–6 antennae of both I and II. These are then used in combination with molecular orbital calculations to define the solution conformation(s) of each linkage in turn. Molecular dynamics simulations for these two types of linkage then allow the relevance of these conformations to be assessed.

Solution Conformations of Manα1–2Manα Linkages. Cross-sections through the NOESY spectrum of I (τ_m = 250 ms) defined interresidue NOE's between residues Man-D_1 and Man-C, Man-C and Man-4, Man-D_2 and Man-A, and Man-D_3 and Man-B. These NOE's could be quantified as described previously (Homans et al., 1987) to define the solution conformation of each Manα1–2Manα linkage. For example, the NOE linking Man-A H1 to Man-D_2 H5 could be quantified by comparison with the intraresidue NOE linking Man-A H1 to Man-A H2. Similarly, an NOE linking Man-D_2 H1 to Man-A H2 was quantified by reference to the NOE linking Man-D_2 H1 to Man-D_2 H2 (Figure 2). The measured relative magnitudes, computed internuclear distances, and ϕ and ψ values are shown in Table I. Similar connectivities across the remaining three Manα1–2Manα linkages were found to generate identical internuclear distances within experimental error, which implies that all four Manα1–2Manα linkages exist in similar conformations in solution (ϕ = −20°, ψ = −160°).

In order to determine whether the experimentally derived conformer is energetically favorable, a series of in vacuo potential energy calculations on Manα1–2Manα were computed by molecular orbital techniques (see Materials and Methods). First, the global minimum conformation was calculated by independent optimization of all bond lengths, bond angles, and dihedral angles of Manα1–2Manα, resulting in a conformation about the glycosidic linkage given by ϕ = +63 and ψ = 150°. However, the theoretical minimum energy conformer is stabilized by a hydrogen bond linking the aglyconic H′6 to O5 of the glycon. In previous investigations (Homans et al., 1986, 1987), we have found that conformers that are stabilized by interresidue hydrogen bonds in vacuo are not populated significantly in solution, since hydrogen bonding to solvent water is statistically more probable. It is thus necessary to examine whether alternative conformers are populated in the absence of the hydrogen bond described above. Accordingly, the calculation was repeated with the dihedral angle O6–C6–C5–H6 of the aglycon fixed at 180° such that the intraresidue hydrogen bond could not exist. A new minimum energy conformer was found at ϕ = 0° and ψ = −160° (Table I). Clearly, the newly defined energy minimum is in close agreement with that of the experimentally derived conformer (Table I). Finally, in order to determine whether the exper-

Table I: NOE's, Internuclear Distances, and ϕ and ψ Values for Compounds I and II

linkage	connectivity	relative magnitude	distance	ϕ (deg), ψ (deg)
	Compound I			
Manα1–3Manβ				
	4-H1, 4-H2	1.00	2.62	
	4-H1, 3-H2	0.40	3.05	+30, −140[c]
	4-H1, 3-H3	4.00	2.08	
	3-H2, 4-H1	0.34	3.03	+50, −140[d]
Manα1–2Manα				
	A-H1, A-H2	1.00	2.64	
	A-H1, D_2-H5	1.30	2.53	−20, −160[c]
	D_2-H1, D_2-H2	1.00	2.63	
	D_2-H1, A-H2	2.08	2.33	0, −160[d]
Manα1–3Manα				
	A-H1, A-H2	1.00	2.65	
	A-H1, 4′-H3/H4[a]	2.60	2.26	−10, −160[c]
	4′-H_2, 4′-H3/H4[a]	1.00	2.46	
	4′-H_2, A-H5	0.60	2.68	+18, −170[d]
Manα1–6Manα				
	B-H1,B-H2	1.00	2.63	
	B-H1, 4′-H6	2.30	2.29	+175, −140[c]
	B-H1, 4′-H6′	1.00	2.63	−120, −165[d]
Manα1–6Manβ				
	4′-H1, 4′-H2	1.00	2.63	
	4′-H1, 3-H6	1.30	2.52	−170, −170[c]
	4′-H1, 3-H6′	0.70	2.79	−140, −170[d]
	Compound II			
Manα1–3Manβ				
	4-H1, 4-H2	1.00	2.62	
	4-H1, 3-H2	0.38	3.07	+30, −140[c]
	4-H1, 3-H3/H4[a]	4.00	2.08	
	3-H2, 4-H1	0.32	3.06	+50, −140[d]
Manα1–3Manα				
	A-H1, A-H2	1.00	2.65	
	A-H1, 4′-H3/H4[a]	2.50	2.27	−10, −160[c]
	4′-H2, 4′H3	1.00	2.46	
	4′-H2, A-H5	0.60	2.68	+18, −170[d]
Manα1–6Manα				
	B-H1, B-H2	1.00	2.63[b]	
	B-H1, 4′-H6	2.00	2.34[b]	+180, −140[e]
	B-H1, 4′-H6′	1.00	2.63[b]	−120, −165[d]
Manα1–6Manβ				
	4′-H1, 4′-H2	1.00	2.63	
	4′-H1, 3-H6	2.73	2.22	+170, −140[c]
	4′-H1, 3-H6′	0.80	2.73	−140, −170[d]

[a] NOE's measured from total integrated intensity of complex multiplet. [b] Approximate values due to resonance overlap. [c] Experimental Values. We estimated an error of ±0.1 Å in distance measurements, giving an error of <±15° in ϕ and ψ. [d] Theoretical values.

imentally and theoretically defined stable conformer was unique, the potential surface of Manα1–2Manα was calculated by independent variation of ϕ and ψ in 30° steps. The dihedral angle H′3–O3–C3–C4 of the glycon was simultaneously optimized at each step to exclude the possibility of steric hindrance by H′3 of this residue. The resulting potential surface is shown in Figure 3a. The experimentally derived conformer exists in a single deep potential well, which strongly suggests that the corresponding ϕ and ψ values correctly describe a unique solution conformation that is similar in all four Manα1–2Manα linkages of compound I (Table I).

Solution Conformations of Manα1–3Manβ and Manα1–3Manα Linkages. The solution conformations of the Manα1–3Manβ linkages in both I and II have been described previously (Homans et al., 1987). For convenience, the NOE values, internuclear distances, and both theoretical and experimental ϕ and ψ values obtained in that study are reproduced in Table I.

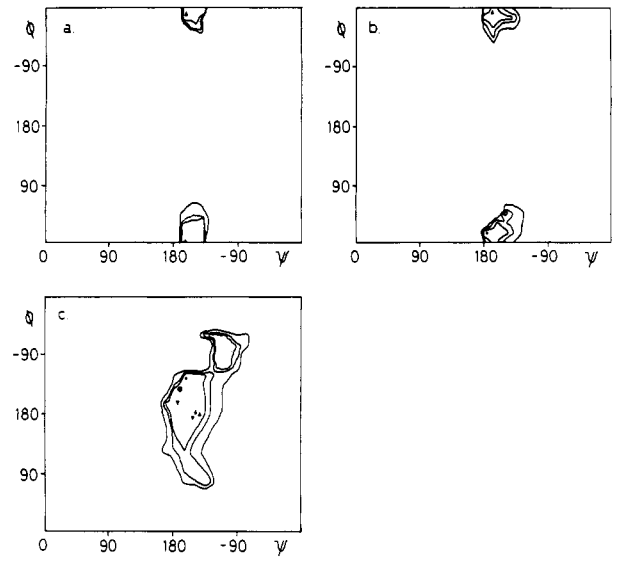

FIGURE 3: Potential surfaces generated by MNDO methods (see text) for (a) Manα1-2Manα, (b) Manα1-3Manα, and (c) Manα1-6Manα. In (a) and (b), experimental and theoretical ϕ and ψ values are denoted (△) and (+), respectively. In (c), the symbols refer to the following: (+) theoretical values for Manα1–6Manα; (⊕) theoretical values for Manα1–6Manβ; (△) experimental values for Manα1–6Manα linkage in compound I; (▽) experimental values for Manα1–6Manβ linkage in compound I; (▲) experimental values for Manα1–6Manα linkage in compound II; (▼) experimental values for Manα1–6Manβ linkage in compound II.

The NOE connectivities observed across the Manα1–3Manα linkage in I were found to be qualitatively different from those observed across the Manα1–3Manβ linkage (Homans et al., 1987). The relevant cross-sections from the NOESY spectrum (τ_m = 250 ms) are shown in Figure 2. Cross-peak intensities were quantified by analogous methods to those described for the Manα1–2Manα linkages, and the resulting NOE magnitudes, computed internuclear distances, and ϕ and ψ values are included in Table I. In addition, an analogous series of molecular obital calculations were performed on Manα1–3Manα. The global minimum energy configuration (ϕ = +18°, ψ = −170°) was found to be in good agreement with the experimentally derived values of ϕ and ψ. In order to locate possible additional stable conformers, ϕ and ψ were varied in 30° steps with independent optimization of the dihedral angle H′4–O4–C4–C5 of the glycon, to account for possible steric hindrance to rotation due to H′4. The resulting potential surface (Figure 3b) was found to define a single deep potential well, which again suggests that the experimentally derived ϕ and ψ values describe an unique solution conformation for the Manα1–3Manα linkage in compound I. The solution conformation about the Manα1–3Manα linkage in II was derived by analogous means and was found to be identical with that in I within experimental error (Table I).

Solution Conformations about Manα1–6Manα and Manα1–6Manβ Linkages. Cross-sections through the NOESY spectrum of compound I (τ_m = 250 mS) that define interresidue connectivities across the Manα1–6Manβ and Manα1–6Manα linkages are shown in Figure 2. Although these are qualitatively similar to those recorded for compound II (data not shown), there are quantitative differences in the case of the Manα1–6Manβ linkage (Table I). This suggests that the solution conformation about this linkage is different in each compound. In an earlier study, we found that the rotamer distributions about the C5–C6 bond of Man-3 were different in the two compounds (Homans et al., 1986). In the case of compound II conformational averaging between ω =

−60° and 180° occurs, whereas in I ω is restricted to 180°. It is therefore perhaps not surprising that the solution conformations of the corresponding glycosidic linkages are different. Quantitation of the NOE's (Table I) defined conformations for the Manα1–6Manβ linkages in both compounds with the ϕ and ψ values shown in Table I. The ϕ and ψ values for the Manα1–6Manα linkage were defined in each compound by similar means.

The global minimum energy conformations for both Manα1–6Manα and Manα1–6Manβ were found to be similar. In the case of the Manα1–6Manα linkage, the global minimum that was initially calculated was stabilized by a hydrogen bond linking H′6 of the aglycon to O1 of the glycon. By similar arguments to those invoked in discussion of the Manα1–2Manα linkages, together with the fact that O1 of the glycon is in glycosidic linkage in both compounds I and II, this conformer was rejected in favor of the minimum energy conformer obtained when this hydrogen bond was not allowed to form (H′6–O6–C6–C5 for the aglycon = 180°). The values of ϕ and ψ corresponding to this minimum energy conformer are shown in Table I, together with those computed for Manα1–Manβ. The potential surface obtained upon independent variation of ϕ and ψ in Manα1–6Manα is shown in Figure 3c. The potential surface for Manα1–6Manβ was not significantly different (data not shown). while the experimentally derived ϕ and ψ values for the Manα1–6Manβ and Manα1–6Manα linkages were found to lie in a low-energy region of the potential surface, these were all found to be significantly different from the corresponding minimum energy conformers (Figure 3c and Table I), with the possible exception of the Manα1–6Manβ linkage of compound I. Since the minimum energy well for both 1–6 linkages is found to be shallow in comparison with those computed for Manα1–2Manα, Manα1–3Manα, and Manα1–3Manβ, it is necessary to consider the possibility that the NMR-derived conformations represent an averge over a number of discrete alternative conformations that can theoretically exist within the bounds of the minimum energy well. Indeed, this is also true of NMR measurements upon Manα1–3Manα, Manα1–3Manβ, and Manα1–2Manα glycosidic linkages, but in these cases the minimum energy well is deep, and the torsional oscillations should thus be restricted to a narrow range about a single conformer. Obviously, since the NOE data *can* be interpreted in terms of stable conformers about both Manα1–6Manα and Manα1–6Manβ linkages, it is impossible to distinguish between these possibilities from NOE measurements alone. We therefore use the molecular dynamics approach (see Materials and Methods) in an attempt to effect a comparison between the various glycosidic linkages of the magnitudes of the torsional fluctuations implied from the energy bounds of the corresponding potential surfaces.

Simulation of Molecular Dynamics Trajectories. In vacuo simulations were performed for the disaccharides Manα1–3Manβ and Manα1–6Manα, each of which is representative of a glycosidic linkage that is defined in terms of a deep potential well and a shallow potential well, respectively. The global minimum energy geometries of each disaccharide were used as input to the simulation, which proceeded in two parts. In an initial equilibration step, the system was coupled to a thermal bath at 300 K with a coupling constant of 0.1 ps, followed by 2-ps simulation with a time step of 2 fs. Second, the simulation was run for a further 10 ps with the coordinates and velocities at the end of equilibration period as input.

Following the molecular dynamics simulation, coordinates were derived for the "average structure" over the 10-ps simulation. In addition, the rms deviations of each atom over the 10-ps period were calculated for each disaccharide, and these data are shown in Figure 4. Average coordinates were also

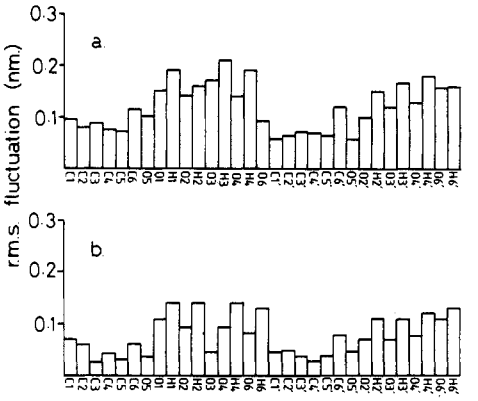

FIGURE 4: Root mean square fluctuations (nm) for each atom during the 10-ps molecular dynamics simulation of (a) Manα1–6Manα and (b) Manα1–3Manβ. The nomenclature used for each atom is described under Materials and Methods.

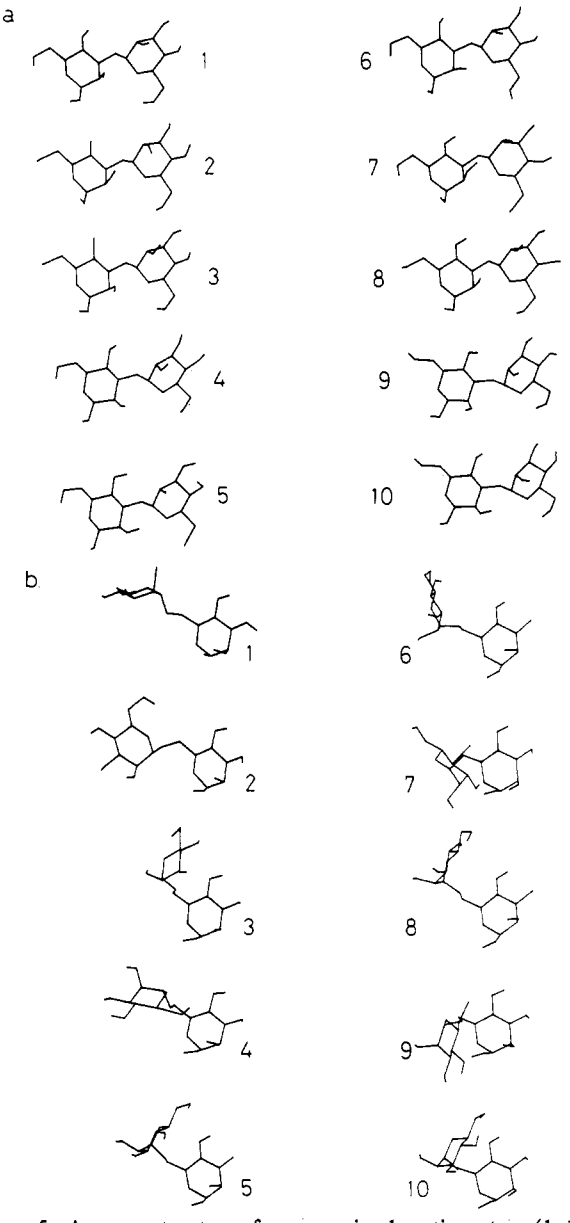

FIGURE 5: Average structures for successive 1-ps time steps (1–10) during the 10-ps molecular dynamics simulations of (a) Manα1–3Manβ and (b) Manα1–6Manα.

Table II: ϕ, ψ, and ω Values for Each 1-ps Average of the Molecular Dynamics Simulations of Manα1–3Manβ and Manα1–6Manα

	Manα1–3Manβ		Manα1–6Manα		
time (ps)	ϕ (deg)	ψ (deg)	ϕ (deg)	ψ (deg)	ω (deg)
1	+18	−148	+124	−146	−30
2	+2	−143	+76	−157	−90
3	+26	−143	+177	−163	+172
4	+48	−113	+152	−80	+192
5	+40	−114	+159	−130	+180
6	+26	−141	+158	−158	+183
7	+3	−159	+115	−122	+180
8	+21	−153	+169	−152	+180
9	+41	−88	+145	−85	+186
10	+39	−92	+158	−150	+183

generated for ten successive 1-ps intervals during the simulations, and the average structures at these successive intervals are shown in Figure 5.

Inspection of Figure 4 shows that for each disaccharide the hydroxyl protons exhibit the greatest freedom of motion. This is due to extensive freedom of motion about the respective C–O bonds, which can clearly be seen in Figure 5. In contrast, the glycosidic oxygen, the anomeric carbons of the aglycon, and C3 of the glycon (Manα1–3Manβ) or C6 of the glycon (Manα1–6Manα) are more restrained. However, the α1–6 glycosidic linkage is considerably more disordered than the α1–3 linkage. Once again this may clearly be seen in qualitative terms from Figure 5. Quantitatively, an estimate of the torsional fluctuations in ϕ and ψ can be had by measuring these parameters at each 1-ps interval. In the case of the Manα1–3Manβ linkage, these fluctuations were each restricted to ±20° with occasional fluctuation to twice this value, over the course of the simulation. In contrast, for the Manα1–6Manα linkage, the fluctuations were much larger, indicating a much greater degree of flexibility (Table II).

The relevance of the simulated parameters can be seen by comparison of the average structure over the 10-ps simulation with the experimentally derived conformers. For each disaccharide, the ϕ and ψ values that define the conformation of the glycosidic linkage of the simulated average structure are shown in Table III. These are compared with the NMR-derived values for the Manα1–3Manβ, Manα1–6Manα, and Manα1–6Manβ linkages in both structure I and structure II. Also, to account for the r^{-6} weighting of NOE-derived "average" structures, a theoretical set of NOE's were computed for each 1-ps time step during the simulation. These were calculated by measurement of internuclear distances from the computed geometry at each time step, which were then interpreted in terms of NOE values with the relevant intraresidue NOE's in Table I as a reference. A linear average of these values then provides an estimate of the ϕ and ψ values that would theoretically be obtained from NOE measurements over the 10-ps average (i.e., an "apparent" average). These values are included in Table III. A more exact estimate, which would be had by considering a large number of smaller time steps, is prohibitively time consuming. In the case of the Manα1–3Manβ linkage, the simulated average structure gives theoretical NMR-derived ϕ and ψ values that are in good agreement with those derived experimentally in each compound. In addition, the fluctuations in ϕ and ψ are in good agreement with those predicted on the basis of the statistical mechanical procedure used to define the bounds of the minimum energy well (Richards & Ganellin, 1974). Both the simulated average conformation and the NMR-derived conformation are thus in good agreement with the global minimum (Table I). These results strongly suggest that the Manα1–3Manβ linkage is restrained in the calculated potential well, with torsional fluctuations of approximately ±20° on the picosecond time scale.

In contrast, as described earlier, the experimental NMR-derived conformations about α1–6 linkages in structures I and II are generally not in good agreement with the global minimum. However, in the case of structure II, the theoretical NMR-derived average conformations of the Manα1–6Manα and Manα1–6Manβ linkages agree more closely with the experimental NMR-derived conformations. These data, taken together with the nature of the potential wells for these linkages, suggest that both the Manα1–6Manα and Manα1–6Manβ linkages are disordered in solution and that the experimental NMR-derived conformation represents an average structure that spans the conformational space defined in Figure 3c. By a similar argument, the NMR-derived ϕ and ψ values for the Manα1–6Manα linkage of I may be interpreted in terms of an average structure over large torsional fluctuations of ϕ and ψ. However, the theoretical NMR-derived average values of ϕ and ψ for the Manα1–6Manβ linkage in I are not in such good agreement with the experimental NMR-derived values. Since the latter are in better agreement with the global minimum ϕ and ψ values, this suggests that the Manα1–6Manβ linkage is more restrained and exists with an average conformation that is close to the global minimum. In view of the fact that ω is restricted to 180° at the Manα1–6Manβ linkage of compound I, this indicates that the Manα1–6Manβ antenna as a whole is restrained.

Discussion

The results of this study indicate that the Manα1–3Manβ linkage in structures I and II exists in solution with an average conformation that is well characterized both from NMR measurements and by molecular dynamics simulation. However, in view of the narrow torsional oscillations about this average, which are estimated at ±20° maximum, the Manα1–3Manβ linkage may be considered as highly restrained in each structure. For this reason the experimentally derived ϕ and ψ values are in excellent agreement with the global minimum derived from molecular orbital calculations. The restrained nature of the Manα1–3Manβ linkage is in fact inferred from the depth of the potential well. Since similar

Table III: Theoretical and Experimental Values for ϕ and ψ in the Linkages Shown (See Text)

			NMR					
	MD av		exptl		calcd		global minimum	
linkage	ϕ (deg)	ψ (deg)	ϕ (deg)	ψ (deg)	ϕ (deg)	ψ (deg)	ϕ (deg)	ψ (deg)
Manα1–3Manβ^a Manα1–3Manβ^b	+26	−130	+30	−140	+40	−140	+50	−140
Manα1–6Manα^a Manα1–6Manα^b	166	−136	+175 +180	−140 −140	+170	−125	−120	−165
Manα1–6Manβ^a Manα1–6Manβ^b	166	−136[c]	−170 +170	−170 −140	+170	−125	−140	−170

[a] For compound I. [b] For compound II. [c] Assumed equivalence with Manα1–6Manα.

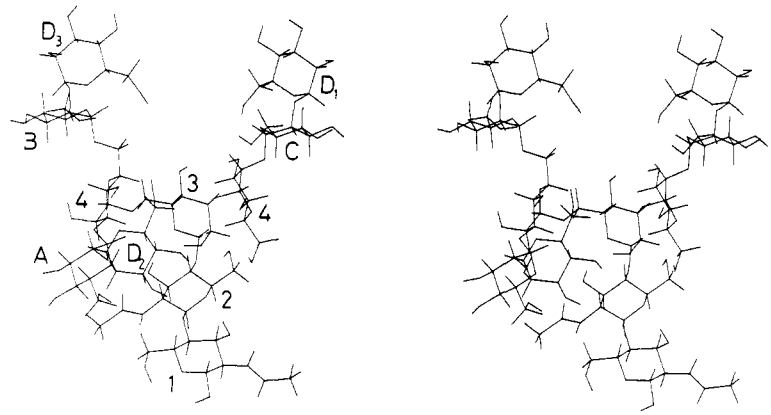

FIGURE 6: Overall conformation of structure I from experimental ϕ and ψ values derived in this study. The Manα1–6Manα linkage is disordered and in this figure is presented in the theoretical average conformation ϕ, ψ = 166°, −136° (Table III). In contrast, the Manα1–6Manβ linkage is restrained and is presented in the NMR- derived configuration, ϕ, ψ = −170°, −170°.

potential surfaces were generated for the Manα1–3Manα and Manα1–2Manα linkages with a single deep potential well in each case, we may conclude that these linkages are also highly restrained.

In contrast, the potential surfaces for Manα1–6Manα and Manα1–6Manβ were found to define a shallow, diffuse potential well in each case. The experimentally derived average conformations for these linkages in compounds I and II were not in good agreement with the global minimum energy conformers, with the exception of the Manα1–6Manβ linkage of I. Molecular dynamics simulations suggest that both Manα1–6Manβ and Manα1–6Manα linkages are disordered, indicating that the NMR-derived average structure is subject to large torsional fluctuations in ϕ and ψ. However, in the light of previous investigations (Homans et al., 1986), together with the above-mentioned differences, the Manα1–6Manβ linkage in I is clearly more restrained.

The above conclusions indicate that it is not accurate to refer to a single overall solution conformation for compound I or II. However in the case of the majority of glycosidic linkages, because torsional oscillations occur over a narrow range, the representation of an unique conformation is still useful in forming a picture of the preferred orientation. As an example, a representative overall conformation of compound I is shown in Figure 6. We note though that in the case of the Manα1–6Manα linkage in both compounds and the Manα1–6Manβ linkage in compound II, conformational averaging occurs. Despite this, the experimental NMR-derived average values of ϕ and ψ for these linkages can be useful parameters even in the presence of large amplitudes of motion, as can be seen from a comparison of columns 1, 3, and 4 in Table III. In theory, the experimentally derived ϕ and ψ values could give a completely false impression of the true average structure due to the r^{-6} dependence of the NOE. The fact that they do not is due to near equivalence of the MD average (column 1) and the apparent average (column 3). This in turn is a function of the motion, i.e., conformers with close approach of the aglyconic H1 atom to H6 or to H6′ having similar probability. Under alternative motional characteristics NOE measurements about 1–6 linkages may not in general reflect the true average structure and should therefore be interpreted with caution.

In light of our results it is interesting to note, on the basis of the "anomerization effect" (Vliegenthart et al., 1983) for a structure similar to I but missing the reducing terminal GlcNAc (GlcNAc1), that the Manα1–6Manβ antenna en bloc lies close to GlcNAc2 of the core. The NMR-derived ϕ and ψ values in compound I show that the Manα1–6Manβ antenna maps a conformational space, which is in the vicinity of the core (Figure 6), but it is not possible from the present data to determine whether any transient arm-core interactions exist.

The results described in the present study show that oligosaccharides can have joint flexibility/rigidity of their conformations. The precise functions of this duality is unknown, but one possibility is that it is important for the interaction of an oligosaccharide with its attached protein. The best characterized example of this is immunoglobulin G, which contains complex-type oligosaccharides and in which extensive interactions occur between the protein and the α1–6 antenna (Deisenhofer, 1981). The orientation of the Manα1–6Manβ linkage in this glycoprotein is defined by ϕ = 170° and ψ = −170°. This conformation lies within the minimum energy bounds of Manα1–6Manβ (Figure 3c), which suggests that the oligosaccharide–protein interaction does not result in a "strained" orientation of the α1–6 antenna. On this basis alone therefore the creation of an oligosaccharide–protein surface is not energetically unfavorable.

Registry No. I, 71246-55-4; II, 66091-47-2; Manα1–3Manβ, 50499-34-8; Manα1–2Manα, 50271-62-0; Manα1–3Manα, 50499-35-9; Manα1–6Manα, 50271-70-0; Manα1–6Manβ, 82729-73-5.

REFERENCES

Biswas, M., Sekharudu, Y. C., & Rao, V. S. R. (1987) *Carbohydr. Res. 160*, 151.

Bock, K., Arnarp, J., & Lonngren, J. (1982) *Eur. J. Biochem. 129*, 171.

Brisson, J.-R., & Carver, J. P. (1983a) *Biochemistry 22*, 3671.

Brisson, J.-R., & Carver, J. P. (1983b) *Biochemistry 22*, 3680.

Deisenhofer, J. (1981) *Biochemistry 20*, 2361.

Dewar, M. J. S., & Stewart, J. J. P. (1986) *AMPAC, QCPE Bull. 506*.

Dorland, L., van Halbeek, H., Vliegenthart, J. F. G., Lis, H., & Sharon, N. (1981) *J. Biol. Chem. 256*, 7708.

Hoch, J. C., Dobson, C. M., & Karplus, M. (1985) *Biochemistry 24*, 3831.

Homans, S. W., Dwek, R. A., Fernandes, D. L., & Rademacher, T. W. (1982) *FEBS Lett. 150*, 503.

Homans, S. W., Dwek, R. A., Boyd, J., Mahmoudian, M., Richards, W. G., & Rademacher, T. W. (1986) *Biochemistry 25*, 6342.

Homans, S. W., Dwek, R. A., & Rademacher, T. W. (1987) *Biochemistry* (in press).

Jardetzky, O., & Roberts G. C. K. (1981) *NMR in Molecular Biology*, Academic, New York.

Liang, C.-J., Yamashita, K., & Kobata, A. (1980) *J. Biochem. (Tokyo) 88*, 51.

Paulsen, H., Peters, T., Sinnwell, V., Lebuhn, R., & Meyer,

B. (1984) *Liebigs Ann. Chem. 5*, 951.
Paulsen, H., Peters, T., Sinnwell, V., Heume, M., & Meyer, B. (1986) *Carbohydr. Res. 156*, 87.
Van Gunsteren, W. F., & Berendsen, H. J. C. (1977) *Mol. Phys. 34*, 1311.
Van Gunsteren, W. F., & Karplus, M. (1982) *Macromolecules 15*, 1528.
Van Gunsteren, W. F., Kaptein, R., & Zuiderweg, E. R. P. (1983) *NATO/CECAM Workshop of Nucleic Acid Conformation/Dynamics*, Orsay, p 79.
Vliegenthart, J. F. G., Dorland, L., & van Halbeek, H. (1983) *Adv. Carbohydr. Chem. Biochem. 41*, 209.
Wüthrich, K., Wider, G., Wagner, G., & Braun, W. (1982) *J. Mol. Biol. 155*, 311.

Solution Conformation of the Branch Points of N-Linked Glycans: Synthetic Model Compounds for Tri′-Antennary and Tetraantennary Glycans†

D. A. Cumming,‡ R. N. Shah,‡ J. J. Krepinsky,§ A. A. Grey,∥ and J. P. Carver*,‡
Departments of Medical Genetics and Medical Biophysics, University of Toronto, Ludwig Institute for Cancer Research, and Toronto Biomedical NMR Centre, Toronto, Ontario, Canada M5S 1A8

Received May 28, 1986; Revised Manuscript Received May 20, 1987

ABSTRACT: The solution conformation of model compounds for the tri′-antennary and tetraantennary (six-arm) branch point of N-linked glycans has been determined through the use of chemical shift, relaxation, and nuclear Overhauser enhancement data. The object was to establish the conformation about the glycosidic linkages in the N-linked substructure GlcNAc(β1,6)[GlcNAc(β1,2)]Man(α)- by estimation of values for the appropriate glycosidic torsional angles. The GlcNAc(β1,6) linkage in a trisaccharide model compound was found to be constrained to a narrow rotameric subpopulation about the substituted Man C5–C6 bond ($\omega = -60°$) and a narrow range of possible $\phi - \psi$ values. Free rotation about the Man C5–C6 bond was obstructed by unfavorable steric interactions between the GlcNAc(β1,6) and GlcNAc(β1,2) residues. A ϕ, ψ value of 55°, 190° was found to be consistent with the NMR data for the GlcNAc(β1,6) linkage. However, the value of ψ appears to be "virtual" in that the molecule is in equilibrium between two different values (90° and 252°). For the GlcNAc(β1,2) linkage, *complete* agreement between all the observed NMR parameters and all the calculated ensemble average values could only be obtained with a set of potential energy functions which included hydrogen bonding. Other choices of potentials yielded calculated values that disagreed with at least two of the observed quantities. As a result, we infer that an interresidue hydrogen bond is formed, and we find it to be between the GlcNAc(β1,2) ring oxygen and the Man C3 hydroxyl. In this conformation the values of ϕ and ψ are restricted to values in the vicinity of 40° and −5°, respectively. This conformation differs from that reported for the same linkage in glycopeptides.

Specification of the solution conformation of glycans has provided valuable insights into their synthesis and biological roles (Lemieux, 1978; Lemieux et al., 1980; Thorgersen et al., 1982; Bock et al., 1982; Carver & Brisson, 1983; Brisson & Carver, 1983a; Rademacher et al., 1983; Montreuil, 1984; Paulsen et al., 1985). Nuclear magnetic resonance spectroscopy (NMR)[1] is especially suited for the determination of the solution conformation of glycans. The NMR parameters of greatest utility to conformational analyses are chemical shifts, coupling constants, relaxation rates, and particularly ^{1}H{^{1}H} NOE's (Lemieux, 1978; Brisson & Carver, 1983b–d; Carver et al., 1987). Unfortunately, direct analysis of the spectra of N-linked glycans is often complicated by spectral overlap and tightly coupled spin systems. To overcome these difficulties, we have previously found it useful to perform conformational analyses on lower molecular weight oligosaccharides, which model substructural elements of larger N-linked glycans (Brisson & Carver, 1983b). This approach has proven particularly useful when specific chemical modification (e.g., deuteriation) of the model compound allows more detailed analysis of complicated spin systems (Cumming et al., 1986). The use of model compounds allows, in NOE experiments, the establishment of a set of expected enhancements. Moreover, an evaluation of the relative contribution of direct and indirect (three-spin) enhancements to the observed NOE signal intensities is facilitated since the NMR spectra of these compounds are intrinsically simpler than those of N-linked glycans.

Thus, prior to embarking on a detailed study of triantennary, tri′-antennary and tetraantennary glycans [for a complete discussion of the various structural classes of N-linked oligosaccharides, see the review of Vliegenthart et al. (1983)], we sought to evaluate the solution conformation of appropriate model compounds. In a forthcoming paper, we will present the results of our study of the conformations about the GlcNAc(β1,2)[GlcNAc(β1,4)]Man(α)- branch point. In this paper, we will present our results on one class of these synthetic compounds, those which model the GlcNAc(β1,2)[GlcNAc-

† This research was supported by Grants MT-3732 and MA-6499 from the Medical Research Council of Canada.
* Address correspondence to this author.
‡ University of Toronto.
§ Ludwig Institute for Cancer Research.
∥ Toronto Biomedical NMR Centre.

[1] Abbreviations: NMR, nuclear magnetic resonance spectroscopy; NOE, nuclear Overhauser enhancement; GlcNAc, 2-acetamido-2-deoxy-D-glucopyranose; Man, D-mannopyranose; FID, free induction decay; SDDS, spin-decoupling difference spectroscopy; T_1, bulk longitudinal relaxation time; Y{X}, NOE observed on nucleus Y upon irradiation of nucleus X.

0006-2960/87/0426-6655$01.50/0 © 1987 American Chemical Society